CELL-TO-MODULE (CTM) ANALYSIS FOR PHOTOVOLTAIC MODULES WITH CELL OVERLAP

Jibran Shahid, Ata Özgün Karabacak, Max Mittag
Fraunhofer Institute for Solar Energy Systems ISE, Heidenhofstr. 2, 79110 Freiburg, Germany
Jibran.Shahid@ise.fraunhofer.de

ABSTRACT: Both, the interconnection of solar cells by ribbons and shingling are known to the solar industry. Typically cells interconnected with ribbons did not overlap while modules with shingled cells did not feature ribbons. A combination of concepts has been presented lately that features ribbons as well as a cell overlap. We analyze this concept for power and efficiency gains and losses from cell to module (CTM) and present models to calculate the CTM-ratio of such photovoltaic modules. We find the efficiency of the PV modules increases by overlapping of the cells, whereas the power of the PV module decreases compared to the conventional module with ribbons and cell spacing.
Keywords: CTM, cell-to-module, shingle-ribbon-interconnection, negative gap, overlap cells, cell spacing, overlap, efficiency analysis, photovoltaic modules

1 INTRODUCTION

The integration of solar cells into PV modules causes different losses and gains which lead to a different PV module output compared to the combined output of the solar cells. [1–6]. These losses and gains can be divided into 15 impact factors [7].

Solar cells are typically interconnected by electrical conductive ribbons [8, 9]. While concepts are known that only contact one side of the solar cell (i.e. IBC, MWT), the majority of PV modules use a front-back interconnection (Figure 1a) [10–12]. A concept that uses a front-back interconnection omits ribbons has been patented in 1960 and is displayed in Figure 1b) [3, 13]. Additionally combination of shingling and traditional ribbon interconnection can be observed in the industry. Manufacturers use (round) wire interconnection [8] but overlap solar cells

In this paper, we present the detailed cell-to-module (CTM) model for overlapped cells. Result of CTM analyses are compared with the other module interconnections as seen in Figure 1. The results of these comparisons are discussed to improve understanding of advantages and disadvantages of the different types of interconnections.

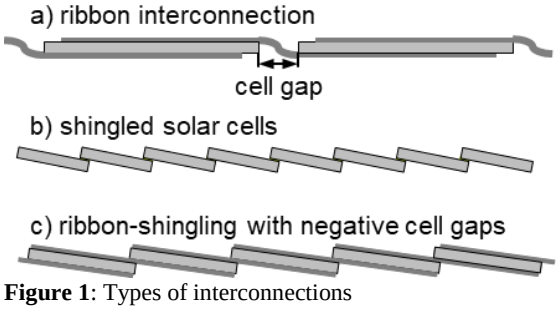

Figure 1: Types of interconnections

2 CELL-TO-MODULE RATIO CALCULATION

General Model

A model to categorize the single CTM-factors and match them with physical loss mechanisms as well as with module components and layers has been presented in previous work and literature [1, 2] We use these models and calculate the module power P_{module} from the CTM-factors k and the sum of the initial solar cell power:

$$P_{module} = \prod_{i=3}^{m} k_i \cdot \sum_{j=1}^{n} P_{cell,j} \quad (1)$$

$$CTM_{power} = \prod_{i=3}^{m} k_i \quad (2)$$

We further extended this model and use it to describe the CTM-ratio of modules with negative cell gap (overlap) and discuss relevant factors in the following section.

CTM- Modelling for Modules with Cell Overlap

A methodology using CTM gain and loss factors k_1-k_{15} build a mechanism that allows the bottom-up prediction of module power and efficiency with given properties of the cells, module materials and the module design. The cell overlap requires an adjustment of the models necessary to calculate the k-factors.

Losses by the inactive module margin and the cell and string spacing areas are described by factors k_1 and k_2. They account for geometrical losses of inactive areas that do not directly contribute to module power but influence efficiency. The latter can be calculated by:

$$\eta_{module} = \frac{P_{module}}{E_{STC} \cdot (A_{margin} + A_{cell\ spacing} + A_{cells})} \quad (3)$$

$$\eta_{module} = \eta_{cell} \cdot (k_1 + k_2 - 1) \cdot \prod_{i=3}^{15} k_i \quad (4)$$

The efficiency depends on the inactive module area share which consists of module margin and cell spacing. The gap between different strings of solar cells defines the cell spacing area for modules with cell overlap. Additional inactive area results from the use of pseudo square solar cells and should also be regarded while calculating $A_{cell\ spacing}$.

Models for the module margin factor k_1 do not change for modules with cell overlap. Therefore the loss factor remains unchanged.

Changes in cell spacing factor k_2 result from omitting the gaps between cells in a string. String spacing still exists. While the factor k_2 is a loss in conventional modules featuring an actual gap between two cells in a string, k_2 might lead to a gain with the consideration of additionally gained area through overlapping.

$$k_2 = 1 - \frac{A_{string\ spacing} - A_{overlap}}{A_{module}} \quad (5)$$

Overlapped area results in a geometrical gain and can be interpreted as saved module area: The module can be made smaller due to the overlap – k_2 therefore is a gain.

Since the overlapping not only covers inactive cell area, there is a power loss from the shading which is considered in factor k_7 (interconnection shading). Cell spacing factor k_2 only considers changes in module area and is based on the assumption of the overlapped region to be entirely inactive. It neglects changes in power as they might occur from shading. It therefore has to be complemented by k_7 which contains such changes in power. The distinction is necessary to achieve a consistent model both for efficiency and power and has been applied before [1].

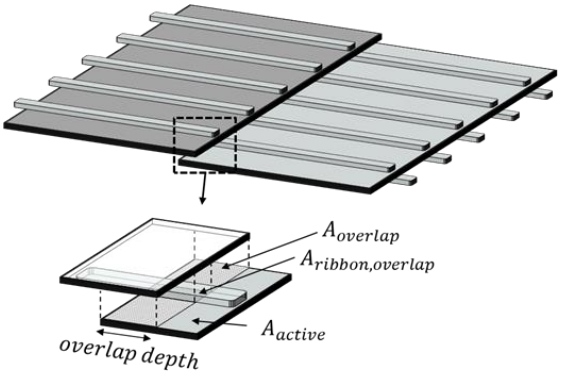

Figure 2: Isometric view of the overlapped cells

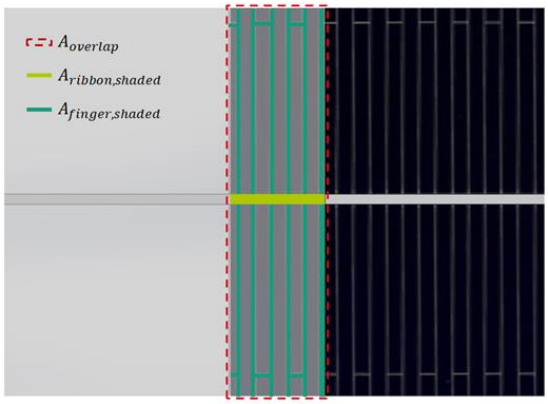

Figure 3: Overlapped area share

By overlapping, active cell area will be partially covered, leading to a reduction of the irradiated area and therefore generated electrical currents and power. We calculate the interconnection shading factor k_7 accordingly, assuming a linear dependency between short circuit current and irradiated cell area.

$$k_7 = 1 - \frac{A_{overlap} + A_{ribbon}}{A_{cell}} - \frac{A_{front\ pad} + A_{ribbon,shaded} + A_{finger,shaded}}{A_{cell}} \quad (6)$$

Figure 2 and **Error! Reference source not found.** visualize the overlapping area, and the ribbon and finger area shaded by overlapping, which are indicated with dashed red rectangle, yellow and green lines respectively.

Factors k_3, k_4, k_5 and k_6 describe the optical behavior (reflection, absorption) of the encapsulation bulk and do not change for modules with cell overlap however their values are expected to be lower in comparison with conventional modules due to the reduction of currents generated in solar cells caused by the shaded region in the overlap.

Cells at one end of the strings are not shaded. However, a typical module contains more than one string and strings are typically interconnected using ribbons as well. For the simplicity, our model assumes the shading of the string connector ribbon to be the same as the shading caused by overlapping. Gains from narrower ribbons or additional losses from increased string ribbon shading are neglected.

The shading of the interconnector is affected by the general shading of the overlapping cell. Since the overlapping cell already shades, the interconnector causes not additional shading. Also other optical factors resulting from the reflections on cell, the finger metallization or the interconnector ribbons are affected. They decrease due to the shading of the top cell. However, the formulation of the respective gain factors k_8, k_9, k_{10} remain unchanged.

Factor k_{11} describes reflection gains from the rear cover of the module (usually a backsheet) [14, 15]. Since a smaller share of backsheet area is visible in modules with overlapping cells, this factor is lower compared to conventional modules. It has been shown that the reflection gain increases with the visible backsheet area and in in previous work it has also been determined that the gains from rear cover reflection are linearly dependent on exposed cell edge length [3].The backsheet coupling factor k_{11} can be therefore easily adjusted by regarding the change in exposed cell edge length compared to a conventional module with a positive cell spacing [15]:

$$k_{11} = I_{SC\ gain} \cdot \frac{l_{cell\ edge}^{overlapped\ interconnection}}{l_{cell\ edge}^{conventional\ module}} \quad (7)$$

The end of each overlapped cell string features a cell with an increased exposed cell edge resulting in a higher gain nearby the edge. However, this additional gain for the last cell in a string will be small, thus we neglect it.

Factor k_{12} describes electrical losses at the cell interconnection. Ohmic losses in ribbons are reduced due to couple of reasons. The current generated in each cell is reduced through additional shading, lower backsheet gains occur and the ribbons interconnecting cells are shorter due to elimination of positive cell spacing (Figure 4). Yet the calculation of the cell interconnection losses is similar to conventional modules using the basic equation:

$$P_{loss} = I^2 \cdot R \quad (8)$$

R is the electrical resistance within a segment of the ribbon (i.e. the distance between two pads on the cell, Figure 4) considering also the parallel interconnection of cell metallization, cell surface and ribbon. The calculation of the total interconnection losses is realized through integration of losses along the ribbon. With Eq. (1) and (2) the loss factor k_{12} can be calculated.

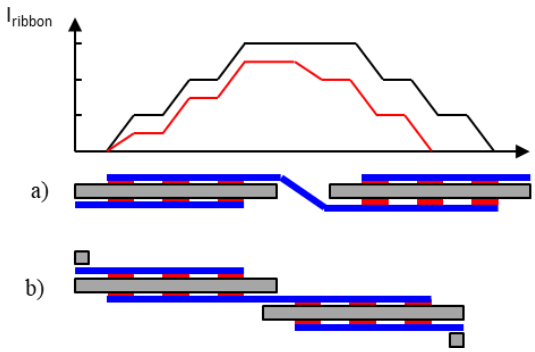

Figure 4: Current commutating through ribbon

Due to the partial shading of the overlap cell, the current generated in the solar cell is reduced resulting in a lower electrical loss in both cell and string interconnections.

Knowing the module topology and the currents flowing through string interconnectors, it is possible to calculate the power loss in the string interconnection. Serial connection of the cell strings is expected to be the most common interconnection method for cell overlap modules as it is in conventional modules. We therefore calculate and add up the string interconnection losses also using Eq. (10) for the single segments of the string interconnector ribbon (Figure 5).

Figure 5: String interconnection and interconnector segments

In solar cell, module material and panel manufacturing imperfections may occur which may lead to deviations in electrical properties. Since all cells are interconnected, electrical mismatch might occur which is considered in k_{14}.

The precision of the cell interconnection is impacting mismatch losses since differences in overlap (Figure 6) result in different shading. The shading results in different currents which lead to increased electrical mismatch of cells in strings.

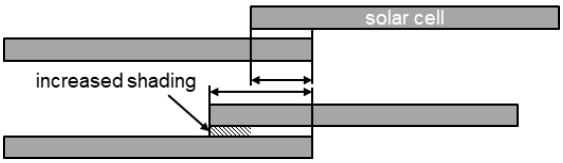

Figure 6: Increased shading of shingled solar cells due to variations in cell placement during manufacturing [3]

Losses in junction boxes and cabling are considered in k_{15}. Despite the consideration of a possible change in the number of junction boxes and bypass diodes resulting from a different module topology in modules with a negative cell gap (i.e. parallel string interconnection), no changes in the modelling of k_{15} are necessary.

All models described above are integrated into the SmartCalc.CTM software [16].We use this software to perform the analysis of the PV module.

3 CTM-ANALYSIS FOR DIFFERENT MODULE DESIGNS

Simulation Setup

In this study, we use 5 busbar full square half cells with a dimension of 79.35 mm x 158.75 mm. The cell efficiency is 21.7% and the total power of cells before encapsulation is 393.63 Wp. The total number of cells in the module is 144. The number of strings is 6 for all types of modules. In order to have the fair comparison between different interconnection, we use the same cells for conventional and overlap module design and also use the base parameters of this cell to create a shingle cell. This way, the input of all modules is the same (ceteris paribus).

For the conventional module, we assume 2 mm cell and string distance. For the shingle cell, we split the 5BB cell into 31.9 mm by 158.75 mm shingle cells. In the shingle module, we use 1 mm cell overlap and 2 mm string distance. Here the total number of cells is 60 per string. For the cell overlap, we apply 1 mm. The total number of cells in overlap module remains same as in conventional module. This way we reduce the total area of the module.

Module materials like glass, EVA and backsheet are assumed to the same for all types of interconnection. Additionally, we have assumed that no loss occur due to cell binning and junction box.

CTM-Analysis for Conventional Modules

After encapsulating, the output efficiency of the reference half-cell PV module is 19.54% and the total module power is 393.6 Wp. **Error! Reference source not found.** shows that k_2 (cell spacing) is -0.68%$_{abs}$. This geometrical loss is significant due to the inactive area of the module resulting from cell spacing. The interconnector shading loss k_7 is -0.09% $_{abs}$ and only caters the losses of ribbon shading in the conventional interconnection design. The cover coupling factor k_{11} (backsheet gains) is 0.28% $_{abs}$. The loss due to cell interconnector k_{12} is 0.07% $_{abs}$. These are the most important factors which will affected by shingling and overlapping. We will discuss them below.

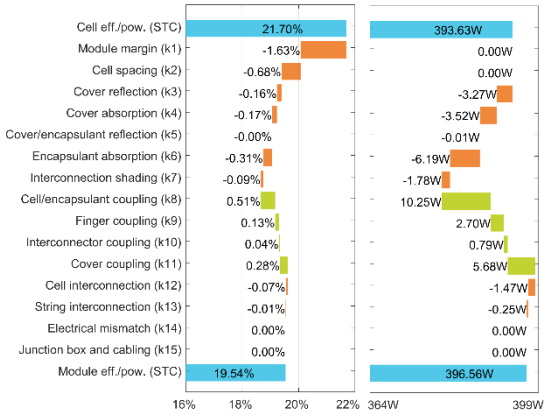

Figure 7: Efficiency and power waterfall diagram of conventional conventional cell module

CTM-Analysis for Shingled Modules

Figure 8 shows the CTM-analysis for a shingled module. The mean efficiency of the shingle cells in the module is 21.70%. The total power of cells before encapsulation is 393.6 Wp. The output efficiency of the shingled module is 20.40% and power is 392.16 Wp. The efficiency is 0.86%$_{abs}$ higher than for the conventional half-cell module. The main difference in efficiency is due to k_2 because of the reduced inactive area. The former loss changed to a gain. As discussed before, this gain is partly compensated in k_7. Here the power loss by cell shading increased to -0.24%$_{abs}$. The cover coupling gain k_{11} decreased due to the reduced visible backsheet area. Besides this we observe that k_{12} is negligible in the shingle module, as the currents are small.

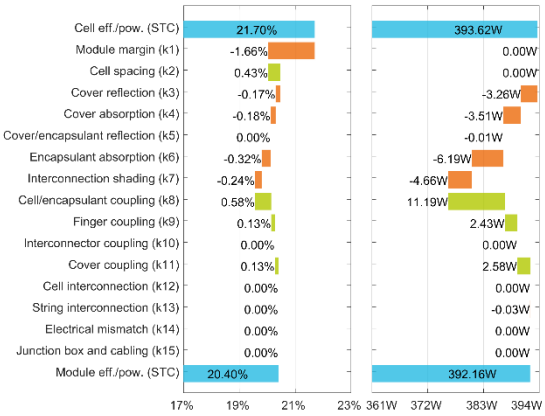

Figure 8: Efficiency and power waterfall diagram of conventional shingle cell module.

CTM-Analysis for Modules with Cell Overlap

After incorporating half cells in the module with cell overlap and ribbon interconnection, the output efficiency of the PV module is found to be 19.81% and the output power is 388.4 Wp (Figure 9). Similar as we have observed in the shingle module, here the inactive area factor k_2 is a gain as well. K_2 has increased compared to the conventional module but it has decreased compared to the shingle module. The difference is caused by the higher number of cells per string in the shingle module resulting in a larger overlapped area.

The highest loss attributed to the cell interconnection (k_7) is obtained in the overlap module because here the losses combine shading and electrical losses in the ribbons. The loss factor k_7 complements the geometrical factor k_2 by considering the shaded active area.

We also observe a loss in k_{11} similar to the shingle module, as the cover coupling gain is reduced to the string spacing area. In the overlap module, we use cell interconnectors to connect all cells but compared to the conventional module, the total length of cell interconnector and the currents are reduced. Therefore we have fewer ohmic losses (k_{12}) compared to the conventional module.

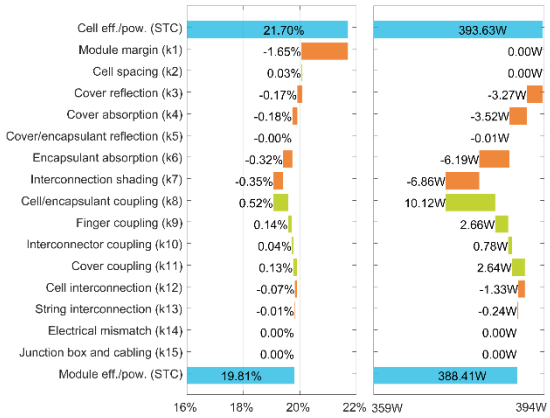

Figure 9: Efficiency and power waterfall diagram of conventional overlap cell module

Comparison of Module Concepts

The CTM-ratio for efficiency of the conventional module is the lowest of all three concepts.

Table 1: Detailed results of the CTM-analysis for a conventional, shingle and overlap module

	Conventional		Shingle		Overlap module	
	E (%)	P (W)	E (%)	P (W)	E (%)	P (W)
Cell	21.7	393.6	21.7	393.6	21.7	393.6
k1	-1.63	0	-1.66	0	-1.65	0
k2	-0.68	0	0.43	0	0.03	0
k3	-0.16	-3.27	-0.17	-3.26	-0.17	-3.27
k4	-0.17	-3.52	-0.18	-3.51	-0.18	-3.52
k5	0	-0.01	0	-0.01	0	-0.01
k6	-0.31	-6.19	-0.32	-6.19	-0.32	-6.19
k7	-0.09	-1.78	-0.24	-4.66	-0.35	-6.86
k8	0.51	10.25	0.58	11.19	0.52	10.12
k9	0.13	2.7	0.13	2.43	0.14	2.66
k10	0.04	0.79	0	0	0.04	0.78
k11	0.28	5.68	0.13	2.58	0.13	2.64
k12	-0.07	-1.47	0	0	-0.07	-1.33
k13	-0.01	-0.25	0	-0.03	-0.01	-0.24
k14	0	0	0	0	0	0
k15	0	0	0	0	0	0
Module	19.54	396.56	20.38	392.2	19.81	388.41
CTM	90.0	100.7	93.9	99.6	91.2	98.7
Δ_{abs}	-2.16	2.93	-1.32	-1.46	-1.9	-5.22

The highest $CTM_{efficiency}$ and the highest efficiency are achieved by shingle module. The $CTM_{efficiency}$ for shingled modules is sensitive to the design of the cell metallization in the overlapped area. Efficiency gains from cell to module are highest, if the shaded area is completely metallized. This also leads to significant gains in our scenario as visible in k_2.

The CTM_{power} of conventional module is the highest for all compared setups. Since k_2 is not part of the analysis for power (purely geometrical impact factor) the negative impact of the inactive area is not relevant for CTM_{power}. Gains from backsheet reflection and now cell shading therefore result in a higher CTM_{power} and the highest module power for the conventional half-cell module.

Table 2: Module dimensions and output

Module	Conventional	Shingle	Overlap
Length (m)	2.02	1.92	1.95
Width (m)	1.01	1.01	1.01
Area (m^2)	2.03	1.93	1.96
Power (W)	396.6	392.2	388.4
(W/m^2)	195.3	203.2	198.2

We calculate the power density (W/m^2) (**Table 2**) to consider the smaller module size of the concepts with overlap and find both overlapping concepts to have a higher values compared to the conventional module.

The module with overlapped cells comes with the advantages and disadvantages of the other two concepts: Being a combination of both concepts, it does neither have the highest efficiency nor power but is in between the two other concepts. Therefore, further work is required and the consideration of additional aspects (i.e. yield or module costs) is required.

4 SUMMARY & CONCLUSION

In this study, we have extended models for the cell-to-module (CTM) analysis to a module concept using overlapped cells and ribbon interconnection. We use these models to perform a comparative CTM analysis.

We find the efficiency of the shingle (20.4%) and overlap module (19.8%) to be higher than for the conventional module (19.5%). This means that the $CTM_{efficiency}$ also increased for these modules. The efficiency for the module with overlap and ribbon interconnection is lower than for the shingled module.

We find the output power of the shingle (392.2 Wp) and overlap module (388.4 Wp) to be lower than the conventional module (396.6 Wp), but if we consider the size of the shingle and overlap module which is smaller than the conventional module. Then the power density W_p/m^2 of the overlapped module is higher than for the conventional module.

We find the concept with overlap and ribbons to not show clear advantages and suggest further analysis considering other parameters such as yield or module costs.

ACKNOWLEDGEMENT

We would like to thank the German Ministry of Economic Affairs and Energy (FKZ 03EE1050) for their funding.

REFERENCES

[1] I. Hädrich *et al.,* "Unified methodology for determining CTM ratios: Systematic prediction of module power," *Sol Energ Mat Sol C*, vol. 131, pp. 14–23, 2014.

[2] H. Wirth *et al., Photovoltaic Modules: Technology and Reliability*. Berlin/Boston: De Gruyter, 2016.

[3] M. Mittag *et al.,* "Cell-to-Module (CTM) analysis for photovoltaic modules with shingled solar cells," in *44th IEEE PV Specialist Conference PVSC*.

[4] M. Mittag *et al.,* "Systematic PV module optimization with the cell-to-module (CTM) analysis software," *Photovoltaics International*, no. 36, pp. 97–104, 2017.

[5] M. Mittag *et al.,* "Techno-Economic Analysis of Half Cell Modules: The Impact of Half Cells on Module Power and Costs," Marseille, France, 2019, pp. 1032–1039.

[6] J. Shahid *et al.,* "A Multidimensional Optimization Approach to Improve Module efficiency, power and costs," in *Proceedings of the 35th European Photovoltaic Solar Energy Conference and Exhibition (EU PVSEC); Brussels, Belgium*, 2018.

[7] M. Mittag *et al.,* "Electrical and thermal modeling of junction boxes," 33rd EUPVSEC, Amsterdam, Netherlands, 2017, pp. 1501–1506.

[8] M. Mittag *et al.,* "Triangular ribbons for improved module efficiency," 32nd EUPVSEC, Munich, Germany, 2016, pp. 169–172.

[9] L. C. Rendler *et al.,* "Mechanical and electrical properties of wave-shaped wires for low-stress interconnection of solar cells," *Sol Energ Mat Sol C*, vol. 176, pp. 204–211, 2018.

[10] J. Walter *et al.,* "Ribbon interconnection of 6" BC-BJ solar cells," *Energy Procedia*, vol. 124, pp. 504–514, 2017.

[11] I. Hädrich *et al.,* "Minimizing the optical cell-to-module losses for MWT-modules," 3rd Silicon PV, Hamelin, Germany, 2013.

[12] ITRPV, "International Technology Roadmap for Photovoltaic (ITRPV): 11th edition, 2019 Results," 2020.

[13] D. C. [J.] Dickson, "Photovoltaic semiconductor apparartus or the like," US 2938938 A, May 31, 1960.

[14] A. Pfreundt *et al.,* "Rapid Calculation of the Backsheet Coupling Gain Using Ray Groups," *32nd European Photovoltaic Solar Energy Conference and Exhibition (EUPVSEC)*, 2018.

[15] M. Mittag *et al.,* "Analysis of backsheet and rear cover reflection gains for bifacial solar cells," *33rd European PV Solar Energy Conference and Exhibition*, vol. 2017.

[16] *cell-to-module.com.* [Online] Available: http://www.cell-to-module.com. Accessed on: Feb. 28 2018.